

Mean first-passage time to a small absorbing target in three-dimensional elongated domains

Denis S. Grebenkov¹ and Alexei T. Skvortsov²

¹*Laboratoire de Physique de la Matière Condensée (UMR 7643), CNRS – Ecole Polytechnique, IP Paris, 91120 Palaiseau, France**

²*Maritime Division, Defence Science and Technology Group, 506 Lorimer Street, Fishermans Bend, Victoria 3207, Australia†*

(Dated: February 16, 2022)

We derive an approximate formula for the mean first-passage time (MFPT) to a small absorbing target of arbitrary shape inside an elongated domain of a slowly varying axisymmetric profile. For this purpose, the original Poisson equation in three dimensions is reduced an effective one-dimensional problem on an interval with a semi-permeable semi-absorbing membrane. The approximate formula captures correctly the dependence of the MFPT on the distance to the target, the radial profile of the domain, and the size and the shape of the target. This approximation is validated by Monte Carlo simulations.

PACS numbers: 02.50.-r, 05.40.-a, 02.70.Rr, 05.10.Gg

Keywords: Mean first-passage time, homogenisation, reactivity, elongated domains, anisotropy

I. INTRODUCTION

The concept of first-passage time, i.e., a time taken for a diffusing particle to arrive at a given location, is very common in describing many natural phenomena. Nowadays it is widely used in chemistry (geometry-controlled kinetics), biology (gene transcription, foraging behavior of animals) and many applications (financial modelling, forecasting of extreme events in the environment, time to failure of complex devices and machinery, military operations), see [1–20] and references therein.

Most former works were dedicated to the *mean* first-passage time (MFPT), which is also related the overall reaction rate on the target region. Since exact formulas for the MFPT are only available for a few special cases of highly symmetric domains (such as sphere or disk), a variety of powerful methods have been developed. In particular, many approximate solutions were derived in the so-called narrow escape limit when the target size goes to 0 [21–35]. While these asymptotic results are valid for generic domains, their accuracy can be considerably reduced when the confining domain is elongated (e.g., a long truncated cylinder or a prolate spheroid). In this case, the target region can still be very small as compared to the diameter of the confining domain (i.e., the size of the domain along the longitudinal direction), but comparable to the size of the domain in the transverse directions. The effect of the confinement anisotropy onto the MFPT was studied in [36]. Recently, we proposed a simple yet efficient method for deriving approximate solutions of the MFPT in elongated domains on the plane [37]. The aim of this paper is to extend this method to three dimensions and to derive a general approximate

formula for the MFPT in an elongated three-dimensional domain with reflecting boundaries. The shape of the domain is assumed to be axisymmetric, smooth and slowly varying in the longitudinal direction (without deep pockets and enclaves), but otherwise general. The target is assumed to be small, but also of an arbitrary shape. We validate our findings by Monte Carlo simulations.

II. APPROXIMATE SOLUTION

We consider an elongated axisymmetric domain of “length” ℓ , which is determined by a smooth profile $r(z)$:

$$\Omega = \{(x, y, z) \in \mathbb{R}^3 : x^2 + y^2 < r^2(z), 0 < z < \ell\}. \quad (1)$$

Throughout the paper, we assume that the aspect ratio r_0/ℓ of the domain (with $r_0 = \max\{r(z)\}$) is small and its boundary profile is smooth, $dr(z)/dz \ll 1$. A small absorbing target is located inside the domain at (x_T, y_T, z_T) , see Fig. 1.

Similar to planar domains [37], the main analytical formula will be derived by employing a three-step approximation. First, the absorbing target is replaced by an absorbing disk of the same trapping coefficient K ; the disk is oriented perpendicular to the symmetry axis of the domain. Far away from the target such a replacement is justifiable because at the distance greater than the size of the target (but still much smaller than $r(z_T)$ and ℓ) the absorption flux can be characterized by the first (monopole) moment of the shape of the target, and this equivalence simply preserves it. The trapping coefficient is proportional to the electrostatic capacitance C of the target, $K = 4\pi DC$, where D is the diffusion coefficient [38, 39]. For a variety of shapes (e.g., sphere, ellipsoid, cube, prism, perturbed axisymmetric shapes, or even some fractals objects), capacitance is well-known or can be accurately estimated from various approximations, see [39–46] and references therein. For a disk of

*Electronic address: denis.grebenkov@polytechnique.edu

†Electronic address: alex.skvortsov@dst.defence.gov.au

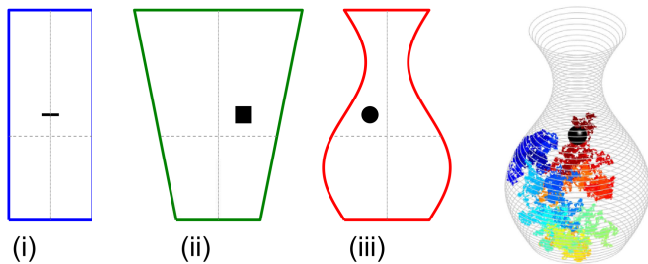


FIG. 1: Projection onto xz -plane of three domains used for Monte Carlo simulations: truncated cylinder, $r(z) = 1$ (i), truncated cone, $r(z) = 1 + z/\ell$ (ii), and a domain with an oscillating profile $r(z) = 1 + \frac{1}{2} \sin(2\pi z/\ell)$ (iii), with $\ell = 5$. Vertical dotted line shows the vertical symmetry axis along z direction ($r = 0$); horizontal dashed line indicates the location of uniformly distributed starting points (at $z = 2$). A target (in black) is located at $(x_T, 0, \ell/2)$: a disk of radius $\rho = 0.2$ with $x_T = 0$ (i), a cube of edge $2\rho = 0.4$ with $x_T = 0.6$ (ii), and a sphere of radius $\rho = 0.2$ with $x_T = -0.4$ (iii). On the right, an example of a simulated trajectory inside the domain with oscillating profile, colored from dark blue to dark red according to elapsed time until the first-passage to the target (black sphere) at the center.

radius a , the capacitance is $(2/\pi)a$ [43]. Knowing the capacitance C of a given target shape, one can thus easily deduce the radius $a = (\pi/2)C$ of the equivalent absorbing disk.

Second, we introduce the semi-permeable and semi-absorbing vertical boundary (membrane) across the domain that passes through the equivalent absorbing disk, i.e., at $z = z_T$, where z_T is the longitudinal target location. In line with the conventional arguments of effective medium theory, the trapping of the target can approximately be captured by means of this boundary with some effective reactivity κ . A similar approach, often referred to as the lump parameter approximation, has been applied in many areas of physics and engineering (effective acoustic impedance of perforated screens [47], effective electric conductance of lattices and grids [48], effective boundary condition for porous materials [49–51]). To relate the effective trapping rate of the membrane with the geometrical setting, we assume that the effective trapping rate of the membrane is equal to the trapping flux of the particles induced by the presence of the target:

$$\kappa = \frac{K(r_T)}{S(z_T)}, \quad (2)$$

where $S(z) = \pi r^2(z)$ is the cross-sectional area at “height” z . We stress that K and thus κ depend on the radial position $r_T = \sqrt{x_T^2 + y_T^2}$ of the target (an equivalent disk) in the cross-section of the domain. In other words, the trapping coefficient $K(r_T)$ of the target inside the confining domain is different from its value K_0 in the open space (when $\Omega = \mathbb{R}^3$). Moreover, it is the latter dependence that determines the MFPT properties. Calculation of the position-dependent trapping coefficient K

is one of the main ingredients of the proposed method. In Appendix, we proposed the following approximation

$$K = K_0 \Psi(a/r(z_T), r_T/r(z_T)), \quad (3)$$

where the function $\Psi(\nu, \eta)$, defined by Eq. (A5), was deduced by interpolating two analytical results for $r_T = 0$ (at the symmetry axis of the domain), and for $r_T = R - a$ (near the domain wall). This function accounts for the relative target size $\nu = a/r(z_T)$ and the relative traversal deviation $\eta = r_T/r(z_T)$ of the target from the center of the domain cross-section.

Third, after its release at some point in the elongated domain, a Brownian particle frequently bounces from the reflecting walls while gradually diffusing along the domain towards the target. The shape of the walls (defined by $r(z)$) can additionally create the so-called entropic drift, which can either speed up or slow down the arrival to the target [4, 11, 12]. In any case, the information about the particle initial lateral location (e.g., across the domain) becomes rapidly irrelevant, and the original MFPT problem, governed by the Poisson equation, is essentially reduced to the one-dimensional problem. While the classical Fick-Jacobs equation determines the concentration of particles averaged over the cross-section of the tube (see [4, 11, 12] and references therein), the survival probability is determined by the backward diffusion equation with the adjoint diffusion operator [52]. In particular, the MFPT $T(z)$ in an elongated domain satisfies [4, 11–13]

$$\frac{d}{dz} \left[S(z) \frac{dT}{dz} \right] = -\frac{S(z)}{D}. \quad (4)$$

As the results of these approximations, the original problem of finding the MFPT to a small target of arbitrary shape in a general elongated domain is reduced to the one-dimensional problem, which can be solved analytically.

We sketch only the main steps of the solution, while the details in a similar case of planar domains can be found in [37]. We search for the solution of Eq. (4) in the intervals $(0, z_T)$ and (z_T, ℓ) . Integrating this equation over z and imposing Neumann (reflecting) boundary conditions at $z = 0$ and $z = \ell$, we get

$$T(z) = \begin{cases} C_- - \int_0^z dz' \frac{V(z')}{DS(z')} & (0 < z < z_T), \\ C_+ - \int_z^\ell dz' \frac{V(\ell) - V(z')}{DS(z')} & (z_T < z < \ell), \end{cases} \quad (5)$$

where $V(z) = \int_0^z dz' S(z')$ is the volume of (sub)domain restricted between 0 and z . The integration constants C_\pm are determined by imposing the effective semi-permeable semi-absorbing boundary condition at the target location $z = z_T$:

$$T(z_T - 0) = T(z_T + 0), \quad (6)$$

$$D \left[\frac{dT}{dz}(z_T + 0) - \frac{dT}{dz}(z_T - 0) \right] = \kappa T(z_T), \quad (7)$$

where κ is given by Eq. (2). The first relation ensures the continuity of the MFPT, whereas the second condition states that the difference of the diffusion fluxes at two sides of the semi-permeable boundary at z_T is equal to the reaction flux on the target (an equivalent disk). The latter flux is proportional to T , with an effective reactivity κ equal to the effective trapping rate of the target, Eq. (2). Finally, substituting Eq. (5) into Eqs. (6, 7), we get the solution of the problem:

$$T(z) = \frac{\ell^2}{D} \left[U_\sigma(z_T/\ell) - U_\sigma(z/\ell) \right] + \frac{\ell}{\kappa} \frac{v(1)}{s(z_T/\ell)}, \quad (8)$$

where we introduced the following dimensionless quantities

$$U_-(\zeta) = \int_0^\zeta d\zeta' \frac{v(\zeta')}{s(\zeta')}, \quad U_+(\zeta) = \int_\zeta^1 d\zeta' \frac{v(1) - v(\zeta')}{s(\zeta')}, \quad (9)$$

with

$$\zeta = z/\ell, \quad S(z) = \pi r_0^2 s(z/\ell), \quad (10)$$

$$V(z) = \pi r_0^2 \ell v(z/\ell), \quad v(\zeta) = \int_0^\zeta d\zeta' s(\zeta'). \quad (11)$$

The index σ in Eq. (8) is the sign of $z - z_T$, i.e., $\sigma = +$ for $z > z_T$, and $\sigma = -$ for $z < z_T$. For a given profile $r(z)$, all these functions can be easily computed either analytically (see examples in Table I), or numerically. In the simplest case of the cylindrical domain, $r(z) = r_0$, one simply gets

$$T(z) = \begin{cases} \frac{z_T^2 - z^2}{2D} + \frac{\ell}{\kappa} & (0 \leq z \leq z_T), \\ \frac{(z - z_T)(2\ell^\kappa - z_T - z)}{2D} + \frac{\ell}{\kappa} & (z_T \leq z \leq \ell). \end{cases} \quad (12)$$

Equation (8) is the main result of the paper. As for the case of planar domains [37], this equation consists of two terms. The first (diffusion) term is independent of the size of the target and is related to the time required for a Brownian particle to arrive at the proximity of the target from its initial position. For this reason, the contribution of this term is small when $z \approx z_T$, i.e. when the particle initial position is near the target. The second (reaction) term in Eq. (8) describes the particle absorption by the target when the particle starts in its vicinity. As it is inversely proportional to the target size, this term dominates in the limit of very small targets. We note that the dependence on the lateral width of the domain comes only through the parameter κ .

In many applications, the starting point is not fixed but uniformly distributed inside the domain. In this case, one often uses to the volume-averaged MFPT

$$\bar{T} = \frac{1}{V(\ell)} \int_0^\ell \pi r^2(z) T(z) dz. \quad (13)$$

Domain	$\rho(\zeta)$	$v(\zeta)$	$U_-(\zeta)$	$U_+(\zeta)$	c_0	$c(\zeta)$
cylinder	1	ζ	$\frac{1}{2}\zeta^2$	$\frac{1}{2}(1-\zeta)^2$	$\frac{1}{3}$	$1-\zeta$
cone	ζ	$\frac{1}{3}\zeta^3$	$\frac{1}{6}\zeta^2$	$\frac{2-3\zeta+\zeta^3}{6\zeta}$	$\frac{1}{15}$	$\frac{1-\zeta}{3\zeta}$
paraboloid	ζ^2	$\frac{1}{5}\zeta^5$	$\frac{1}{10}\zeta^2$	$\frac{3\zeta^5-5\zeta^3+2}{30\zeta^3}$	$\frac{1}{35}$	$\frac{1-\zeta^3}{15\zeta^3}$

TABLE I: Three examples of symmetric elongated domains defined by setting $r(z) = r_0 \rho(z/\ell)$, where $\rho(\zeta)$ is the rescaled radial profile, $\zeta = z/\ell$, ℓ is the length of the domain, $r_0 = \max\{r(z)\}$; $v(\zeta)$ is the rescaled volume in Eq. (11), functions $U_\pm(\zeta)$ are given in Eq.(9). Constant c_0 and function $c(\zeta)$ are given by Eq. (15). Other examples can be deduced from similar expressions for the planar case [37] due to the identity $\rho^2(\zeta) = h(\zeta)$ between the rescaled profile $\rho(\zeta)$ of a three-dimensional domain and the rescaled profile $h(\zeta)$ of the analogous two-dimensional domain.

By substituting Eq. (8) into this expression we arrive at

$$\bar{T} = \frac{\ell^2}{D} (c_0 + c(z_T/\ell)) + \frac{\ell}{\kappa} \frac{v(1)}{s(z_T/\ell)}, \quad (14)$$

with

$$c_0 = \int_0^1 d\zeta \frac{v^2(\zeta)}{v(1)s(\zeta)}, \quad c(\zeta) = \int_\zeta^1 d\zeta' \frac{v(1)}{s(\zeta')}. \quad (15)$$

Note also that

$$U_+(\zeta) = c(\zeta) - (U_-(1) - U_-(\zeta)). \quad (16)$$

III. DISCUSSION

We use Monte Carlo simulations to check the accuracy of the analytical predictions given by Eq. (8) in three geometrical settings illustrated in Fig. 1: (i) a disk of radius ρ in a truncated cylinder; (ii) a cube of edge 2ρ in a truncated cone; and (iii) a sphere of radius ρ in an oscillating profile. The capacitances of these targets are respectively $(2/\pi)\rho$, $(4/3)\rho$ [39, 45], and ρ , from which the radius a of an effective disk takes the values ρ , $(2\pi/3)\rho$ and $(\pi/2)\rho$, respectively. The target is located at $(r_T, 0, \ell/2)$, where $\ell = 5$ is the length of the confining domains. In each simulation run, a particle was released from a random point uniformly distributed in the cross-section at $z_0 = 2$. It undertakes independent Gaussian jumps with the standard deviation $\sigma = \sqrt{2D\delta}$ along each coordinate, where $D = 1$ and $\delta = 10^{-6}$ is the time step. The particle is reflected normally on the boundary of the confining domain. The simulation run is stopped when the particle crossed the target. The first-passage time is estimated as $n\delta$, where n is the number of steps until stopping. The MFPT is obtained by averaging over 1000 runs.

The approximate solution for a truncated cylinder is given in Eq. (12), while the general expression (8) is used for two other domains. In the case of a truncated cone

$r(z) = a + bz$, the functions $U_{\pm}(\zeta)$ can also be found explicitly:

$$U_{-}(\zeta) = \frac{\zeta^2(3 + \alpha\zeta)}{6(1 + \alpha\zeta)}, \quad U_{+}(\zeta) = \frac{(1 - \zeta)^2(3 + 2\alpha - \alpha\zeta)}{6(1 + \alpha\zeta)},$$

with $\alpha = b\ell/a$. In turn, for an oscillating profile, it is easier to calculate $U_{\pm}(\zeta)$ directly from their definition (9) via numerical integration.

Figure 2 presents the MFPT as a function of the radial position r_T of the target in the domain. First of all, one can note the overall agreement between our theoretical predictions and Monte Carlo simulations. Both theory and simulations indicate that the MFPT increases when the target is shifted from the center ($r_T = 0$) towards the boundary of the confining domain ($r_T = 0.8$), even though this effect is weak. For a larger spherical target (panel (a), $\rho = 0.2$), our approximation slightly underestimates the MFPT in the case (iii) of an oscillating domain; the agreement is better for a smaller target (panel (b), $\rho = 0.1$). There are also minor deviations for the case (i) when the disk is close to the boundary. Despite these deviations, we conclude that our three-step approximation accurately captures the properties of the MFPT in elongated domains. Given the simplistic character of this approximation, its accuracy is striking. It is worth stressing that the targets are not too small (e.g., $\rho = 0.2$ is comparable to the minimal radius of $r(0.75\ell) = 0.5$ of the oscillating domain); the domains are not too elongated (e.g., $r_0/\ell = 0.4$ for the truncated cone); and the particles are released not too far from the target (here, $z_T - z_0 = 0.5$ is comparable to the target diameter $2\rho = 0.4$). In other words, even though the assumptions of our approximation are not fully satisfied, its predictions remain in a quantitative agreement with Monte Carlo simulations.

IV. CONCLUSIONS AND PERSPECTIVES

In this paper, we obtained a simple formula (8) for the MFPT to a small absorbing target of an arbitrary shape in an elongated axisymmetric domain with slowly changing boundary profile. This formula expresses the MFPT in terms of dimensions of the domain, the form and size of the absorbing target and its relative position inside the domain. We validated our analytical predictions by numerical simulations and found excellent agreement. Similar to the planar domains [37] the validity of the proposed framework grounded on the condition of slowly changing profile $dr(z)/dz \ll 1$.

A conventional way of improving the proposed approximation is to account for the next order in the perturbation expansion, which entails introduction of the position-dependent diffusion coefficient [4]

$$D \rightarrow \frac{D}{\sqrt{1 + [dr(z)/dz]^2}}. \quad (17)$$

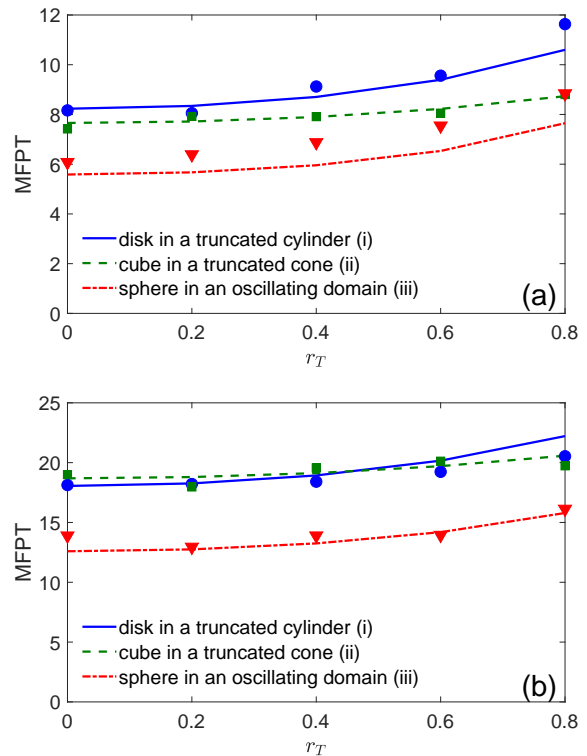


FIG. 2: MFPT as a function of r_T for diffusion towards a target centered at $\mathbf{x}_T = (r_T, 0, \ell/2)$, with $\rho = 0.2$ (a) or $\rho = 0.1$ (b), $D = 1$, $\ell = 5$, the starting point \mathbf{x}_0 is uniform at the cross-section at $z_0 = 2$, in three settings shown in Fig. 1: (i) a disk of radius ρ inside a truncated cylinder of radius 1; (ii) a cube of edge 2ρ inside a truncated cone $r(z) = 1 + z/\ell$; and (iii) a sphere of radius ρ inside an oscillating domain $r(z) = 1 + \frac{1}{2} \sin(2\pi z/\ell)$. Lines show theoretical predictions (8); symbols present the mean values from 1000 realizations obtained via Monte Carlo simulations with the time step $\delta = 10^{-6}$.

We note that under this approximation the results for the cylindrical domain remain unchanged while an extension of the main formula (8) is getting more challenging.

Future work may involve an extension of the proposed framework to more complex geometries (an elongated domain with a compound piecewise profile) or an extension to the slightly bended domain (but still with a circular cross-section). These extensions are straightforward; the latter case reduces to a simple change of the coordinate z in the main equation (8) to the longitudinal curvilinear coordinate along the bended domain. The generalization of Eq. (8) to domains with non-circular cross-section is also possible, but is more involved and would require a substantial refinement of relation (3), while the main Eq. (8) remains valid.

We believe that the proposed expression for the MFPT is a useful tool for some rapid practical estimations as well as for validation of complex numerical models of particle diffusion in geometrically constrained settings.

Acknowledgments

D. S. G. acknowledges a partial financial support from the Alexander von Humboldt Foundation through a Bessel Research Award. A. T. S. thanks Paul A. Martin for many helpful discussions.

Appendix A: Effective trapping coefficient for an absorbing disk inside a tube

We derive an approximate expression for the trapping coefficient K of a small disk of radius a in a reflecting tube with the cross-sectional area $S(z) = \pi r^2(z)$. For planar domains, the expression for K can be deduced analytically [37]. Unfortunately, there is no closed-form analytical solution for K in the case of a general position of the absorbing disk in a three-dimensional tube with reflecting walls (we note that the classical results for the capacitance of a small conductor in a tube [53–55] correspond to the Dirichlet boundary condition boundary condition on the tube wall). Nevertheless, there are some analytical results that can be used to conjecture an accurate interpolating solution.

The expression for K is indeed position dependent: $K = K(r_T, z_T)$. The dependence on z_T is “adiabatic” and comes with the slowly changing profile of the domain, $r(z)$. As a function of r_T , K has a weak maximum at the center of the domain (the most symmetrical configuration) that follows from the symmetry of the problem and general bounds on the capacitance. To capture these properties we can begin with a simple ansatz

$$\frac{K(\nu, \eta)}{K_0} = A(\nu)[1 - B(\nu)\eta^p], \quad (\text{A1})$$

where $K_0 = 8aD$ is the trapping coefficient of a disk of radius a , $\eta = r_T/r(z_T) \leq 1$, $\nu = a/r(z_T) \ll 1$ and parameters $A(\nu)$, $B(\nu)$ and p to be determined.

For $\eta = 0$ (the centered disk) the solution has been derived by Fock [56], from which

$$A(\nu) = \frac{1 + 1.37\nu - 0.37\nu^4}{(1 - \nu^2)^2} \geq 1. \quad (\text{A2})$$

The second parameter, $B(\nu)$, can be found from the situation when the disk touches the wall of the tube. In this case $\eta = 1 - \nu$ and we can write this condition in the form

$$\frac{K}{K_0} = qA, \quad (\text{A3})$$

with some constant factor q . The value of factor q can be deduced from a general scaling argument. It is well known that the capacitance (and hence the trapping rate) scales with the square root of the surface area of conductor (absorber) [39, 44]. So the capacitance of any conductor touching the reflecting wall is approximately $\sqrt{2}/2 \approx 0.71$ of its value at the center of the tube (at $\eta = 0$), which leads to Eq. (A3). This conjecture can also be validated with the analytical results for two touching disks, $q = 3/4$ [57] or $q = 0.74$ [58], and two touching spheres when $q = \ln 2 \approx 0.69$ [39, 59], which are reasonably close. From here we arrive at

$$B(\nu) = \frac{1 - q}{(1 - \nu)^p} > 0. \quad (\text{A4})$$

The value of exponent $p = 2$ can be deduced from comparison with the analytical results for the flux of a monopole source in the tube [51] near the tube center ($\eta = 0$). One can also estimate it directly from numerical simulations.

Combining Eqs. (A1, A2, A4), we get our analytical model (3) for the trapping coefficient, with

$$\Psi(\nu, \eta) = A(\nu)[1 - B(\nu)\eta^2]. \quad (\text{A5})$$

-
- [1] S. Redner, *A Guide to First Passage Processes* (Cambridge University Press, Cambridge, 2001).
- [2] R. Metzler, G. Oshanin, and S. Redner (Eds.) *First-Passage Phenomena and Their Applications* (World Scientific, Singapore, 2014).
- [3] K. Lindenberg, R. Metzler, and G. Oshanin (Eds.) *Chemical Kinetics: Beyond the Textbook* (New Jersey: World Scientific, 2019).
- [4] D. Reguera and J. M. Rubi, Kinetic equations for diffusion in the presence of entropic barriers, *Phys. Rev. E* **64**, 061106 (2001).
- [5] Y. Lanoiselée, N. Moutal, and D. S. Grebenkov, Diffusion-limited reactions in dynamic heterogeneous media, *Nature Commun.* **9**, 4398 (2018).
- [6] D. S. Grebenkov, Paradigm Shift in Diffusion-Mediated Surface Phenomena, *Phys. Rev. Lett.* **125**, 078102 (2020).
- [7] P. Bressloff and S. D. Lawley, Stochastically gated diffusion-limited reactions for a small target in a bounded domain, *Phys. Rev. E* **92**, 062117, (2015).
- [8] M. Reva, D. A. DiGregorio, and D. S. Grebenkov, A first-passage approach to diffusion-influenced reversible binding: insights into nanoscale signaling at the presynapse, *Sci. Rep.* **11**, 5377 (2021).
- [9] D. S. Grebenkov, Universal formula for the mean first passage time in planar domains, *Phys. Rev. Lett.* **117**, 260201 (2016).
- [10] O. Bénichou and R. Voituriez, From first-passage times of random walks in confinement to geometry-controlled kinetics, *Phys. Rep.* **539**, 225-284, (2014).
- [11] P. Kalinay and J. K. Percus, Corrections to the Fick-Jacobs equation, *Phys. Rev. E* **74**, 041203 (2006).
- [12] J. M. Rubi and D. Reguera, Thermodynamics and stochastic dynamics of transport in confined media,

- Chem. Phys. **375**, 518-522 (2010).
- [13] A. E. Lindsay, A. J. Bernoff, and M. J. Ward, First passage statistics for the capture of a Brownian particle by a structured spherical target with multiple surface traps, *SIAM J. Multiscale Model. Simul.* **15**, 74-109 (2017).
- [14] D. Holcman and Z. Schuss, *Stochastic Narrow Escape in Molecular and Cellular Biology* (Springer, Berlin, 2015).
- [15] B. O. Koopman, *Search and Screening: General Principles with Historical Applications* (Pergamon Press, 1980).
- [16] O. Bénichou, C. Loverdo, M. Moreau, and R. Voituriez, Intermittent search strategies, *Rev. Mod. Phys.* **83**, 81 (2011).
- [17] G. Oshanin, O. Vasilyev, P. L. Krapivsky, and J. Klafter, Survival of an evasive prey, *Proc. Nat. Acad. Sci. USA* **106**, 13696-13701 (2009).
- [18] O. Bénichou, D. S. Grebenkov, P. Levitz, C. Loverdo, and R. Voituriez, Optimal Reaction Time for Surface-Mediated Diffusion, *Phys. Rev. Lett.* **105**, 150606 (2010).
- [19] O. Bénichou, C. Chevalier, J. Klafter, B. Meyer, and R. Voituriez, Geometry-controlled kinetics, *Nature Chem.* **2**, 472-477 (2010).
- [20] D. S. Grebenkov, R. Metzler, and G. Oshanin, Strong defocusing of molecular reaction times results from an interplay of geometry and reaction control, *Commun. Chem.* **1**, 96 (2018).
- [21] I. V. Grigoriev, Y. A. Makhnovskii, A. M. Berezhkovskii, and V. Y. Zitserman, Kinetics of escape through a small hole, *J. Chem. Phys.* **116**, 9574 (2002).
- [22] T. Kolokolnikov, M. S. Titcombe, and M. J. Ward, Optimizing the Fundamental Neumann Eigenvalue for the Laplacian in a Domain with Small Traps, *Eur. J. Appl. Math.* **16**, 161 (2005).
- [23] A. Singer, Z. Schuss, D. Holcman, and R. S. Eisenberg, Narrow Escape, Part I, *J. Stat. Phys.* **122**, 437-463 (2006).
- [24] A. Singer, Z. Schuss, and D. Holcman, Narrow Escape, Part II The circular disk, *J. Stat. Phys.* **122**, 465 (2006).
- [25] A. Singer, Z. Schuss, and D. Holcman, Narrow Escape, Part III Riemann surfaces and non-smooth domains, *J. Stat. Phys.* **122**, 491 (2006).
- [26] S. Pillay, M. J. Ward, A. Peirce, and T. Kolokolnikov, An Asymptotic Analysis of the Mean First Passage Time for Narrow Escape Problems: Part I: Two-Dimensional Domains, *SIAM Multi. Model. Simul.* **8**, 803-835 (2010).
- [27] A. F. Cheviakov, M. J. Ward, and R. Straube, An Asymptotic Analysis of the Mean First Passage Time for Narrow Escape Problems: Part II: The Sphere, *SIAM Multi. Model. Simul.* **8**, 836-870 (2010).
- [28] A. F. Cheviakov and M. J. Ward, Optimizing the principal eigenvalue of the Laplacian in a sphere with interior traps, *Math. Computer Model.* **53**, 1394-1409 (2011).
- [29] A. F. Cheviakov, A. S. Reimer, and M. J. Ward, Mathematical modeling and numerical computation of narrow escape problems, *Phys. Rev. E* **85**, 021131 (2012).
- [30] C. Caginalp and X. Chen, Analytical and Numerical Results for an Escape Problem, *Arch. Rational. Mech. Anal.* **203**, 329-342 (2012).
- [31] D. Holcman and Z. Schuss, The Narrow Escape Problem, *SIAM Rev.* **56**, 213-257 (2014).
- [32] J. S. Marshall, Analytical Solutions for an Escape Problem in a Disc with an Arbitrary Distribution of Exit Holes Along Its Boundary, *J. Stat. Phys.* **165**, 920-952 (2016).
- [33] D. S. Grebenkov and G. Oshanin, Diffusive escape through a narrow opening: new insights into a classic problem, *Phys. Chem. Chem. Phys.* **19**, 2723-2739 (2017).
- [34] D. S. Grebenkov, R. Metzler, and G. Oshanin, Towards a full quantitative description of single-molecule reaction kinetics in biological cells, *Phys. Chem. Chem. Phys.* **20**, 16393-16401 (2018).
- [35] D. S. Grebenkov, R. Metzler, and G. Oshanin, Full distribution of first exit times in the narrow escape problem, *New J. Phys.* **21**, 122001 (2019).
- [36] D. S. Grebenkov, R. Metzler, and G. Oshanin, Effects of the target aspect ratio and intrinsic reactivity onto diffusive search in bounded domains, *New J. Phys.* **19**, 103025 (2017).
- [37] D. S. Grebenkov and A. T. Skvortsov, Mean first-passage time to a small absorbing target in an elongated planar domain, *New J. Phys.* **22**, 113024 (2020).
- [38] P. L. Krapivsky, S. Redner, and E. Ben-Naim, *A Kinetic View of Statistical Physics* (Cambridge University Press, 2010).
- [39] A. M. Berezhkovskii and A. V. Barzykin, Simple formulas for the trapping rate by nonspherical absorber and capacitance of nonspherical conductor, *J. Chem. Phys.* **126**, 106102 (2007).
- [40] A. T. Skvortsov and A. M. Berezhkovskii, and L. Dagdug, Trapping of diffusing particles by spiky absorbers, *J. Chem. Phys.* **148**, 084103 (2018).
- [41] P. R. Nair and M. A. Alam, Dimensionally Frustrated Diffusion towards Fractal Adsorber, *Phys. Rev. Lett.* **99**, 256101 (2007).
- [42] N. Landkof, *Foundations of Modern Potential Theory*, (Springer Verlag, Berlin, 1972).
- [43] L. D. Landau, L. P. Pitaevskii, and E. M. Lifshitz, *Electrodynamics of Continuous Media* (Elsevier Science and Technology, 1984).
- [44] Y. L. Chow and M. M. Yovanovich, The shape factor of the capacitance of a conductor, *J. App. Phys.* **53**, 8470-8475 (1982).
- [45] H. J. Wintle, The capacitance of the cube and square plate by random walk methods, *J. Electrostat.* **62**, 51-62 (2004).
- [46] F. Piazza and D. S. Grebenkov, Diffusion-controlled reaction rate on non-spherical partially absorbing axisymmetric surfaces, *Phys. Chem. Chem. Phys.* **21**, 25896-25906 (2019).
- [47] M. J. Crocker, *Handbook of Acoustics* (New York: Wiley, 1998).
- [48] S. Tretyakov, *Analytical Modeling in Applied Electromagnetics* (Boston: Artech House Publishers, 2003).
- [49] D. P. Hewett and I. J. Hewitt, Homogenized boundary conditions and resonance effects in Faraday cages, *Proc. R. Soc. A* **472**, 20160062 (2016).
- [50] J. J. Marigo and A. Maurel, Two-scale homogenization to determine effective parameters of thin metallic-structured films, *Proc. R. Soc. A* **472**, 20160068 (2016)
- [51] P. A. Martin, On Green's function for Laplace's equation in a rigid tube, *Quart. Appl. Math.* **80**, 87-98 (2022).
- [52] C. W. Gardiner, *Handbook of Stochastic Methods for Physics, Chemistry and the Natural Sciences*, (Berlin, Springer, 1985).
- [53] W. R. Smythe, Charged Sphere in Cylinder, *J. Appl. Phys.* **31**, 553 (1960).
- [54] W. R. Smythe, Charged Spheroid in Cylinder, *J. Math. Phys.* **4**, 833 (1963).
- [55] I. C. Chang, and I. Dee Chang, Potential of a Charged

- Axially Symmetric Conductor Inside a Cylindrical Tube, *J. Appl. Phys.* **41**, 1967 (1970).
- [56] V. A. Fock, A theoretical investigation of the acoustical conductivity of a circular aperture in a wall put across a tube, *Doklady Acad. USSR* **31**, 875 (1941).
- [57] V. I. Fabrikant, On the potential flow through membranes, *J. App. Math. Phys. (ZAMP)* **36**, 616-623 (1985).
- [58] W. Strieder, Interaction between two nearby diffusion-controlled reactive sites in a plane, *J. Chem. Phys.* **129**, 134508 (2008).
- [59] J. Lekner, Capacitance coefficients of two spheres, *J. Electrostat.* **69**, 11-14 (2011).